Journal of the Korean Nuclear Society
Volume 23, Number 2, June 1991

Thermal Transient Response of a PWR Pressurizer Vessel Wall for the Inadvertent Auxiliary Spray Transient

Jong Chull Jo, Sang Kyoon Lee and Won Ky Shin
Korea Institute of Nuclear Safety

Jin Ho Cho
Hanyang University

(Received December 4, 1990)

PWR가압기에서 오동작 보조살수 과도시 용기벽의 열적 과도응답

조종철 · 이상균 · 신원기
한국원자력안전기술원

조진호
한양대학교

(1990. 12. 4 접수)

Abstract

Transient response of temperature distributions in a Pressurized Water Reactor (PWR) pressurizer vessel wall for the Inadvertent Auxiliary Spray transient has been analyzed with conservatism accounted for the resulting thermal stresses in the regions of the vessel wall which are wetted by the spray water droplets. In order to determine the forced convective heat transfer coefficient at the inner boundary surface of vessel wall where the droplets impinge on and flow down, the transient temperatures of spray droplets when they reach the inner surface of the vessel wall after travelling from the spray nozzle through the pressurizer interior space occupied with the saturated steam–noncondensable hydrogen gas mixture have been predicted. The transient temperature distributions in the vessel wall have been obtained by using the finite element method, and the typical results have been provided. It has been shown that the results of thermal analysis are consistent with representation of the input transient and have plausible physical meaning.

요 약

가압수형 원자로 가압기의 오동작 보조살수 과도시 용기벽에서의 온도분포에 대한 과도응답을 해석하였으며, 해석은 분무수적으로 젖게되는 용기벽면에서 나타나는 열응력에 대하여 보수적으로 수행되었다. 수적이 부딪혀서 흘러내리는 용기벽의 내부경계면에서 강제대류열전달계수를 결정하기 위하여, 분무수적들이 살수노즐을 떠나 수증기와 비응축성인 수소기체로 이루어진 혼합기로 채워져 있는 가압기 내부공간을 통하여 비행한 후에 용기내부벽면에 도달할 때의 수적들의 과도

온도를 예측하였다. 용기벽에서의 과도온도분포는 유한요소법을 사용하여 구하였으며, 대표적인 결과들을 제시하였다. 열해석의 결과는 입력자료에 대한 묘사와 부합되며, 타당한 물리적 의미를 가짐이 확인되었다.

1. Introduction

During the lifetime of a PWR nuclear power plant, the pressurizer upper head and upper shell are subjected to the various pressure and thermal loads. Therefore, structural integrity of the pressurizer must be justified by a conservative stress analysis which is in compliance with the stress limits and design rules established for the design conditions and the additional conditions[1]. A considerable amount of alternating thermal stresses in the pressurizer upper head and upper shell may be caused by transient thermal loads during the Inadvertent Auxiliary Spray transient, because the temperature of water droplets sprayed from the pressurizer nozzle is lower than for any other spray transient, and thus the impingement of cold droplets on the inner wall surface would cause significant temperature gradients and thermal stresses, in the portions of the vessel wall wetted by the spray droplets, in both radial and axial directions. With regard to nuclear regulation, it is necessary to review the manufacturer s report for the structural adequacy of the pressurizer during the lifetime by performing an audit calculation as accurately as possible in special conditions. In this study, the transient responses of temperature distributions in the pressurizer vessel wall for the Inadvertent Auxiliary Spray transient are analyzed as realistically as possible but with conservatism accounted for the resulting thermal stresses in the upper head and upper shell of the pressurizer. A prerequisite for analyzing the transient reponse of temperature distributions in the vessel wall exposed to spray droplets is a knowledge of the temperature and velocity of impinging fluid, which is used for the determination of forced convective heat transfer coefficient at the inner boundary surface of vessel wall where the spray droplets impinge on and flow down. Thus, it is required to be able to predict the heat and mass transfer rates to a spray droplet from the ambient fluid. Tanaka[2] reported the results of modeling heat transfer rates to a spray droplet under conditions of a loss–of–coolant accident in a light water reactor and developed a computer program CONDENSE, which was designed to calculate the heat and mass transfer rates to both a non–mixing droplet model (in which heat transfer within the droplet is achieved only by conduction) and a complete mixing droplet model (which is considered as lumped system). His model allows for droplet growth due to steam condensation, heat transfer resistance in the condensate film on the droplet surface, temperature dependency on physical properties and the influence of noncondensable air on the mass transfer coefficient. However, the use of Tanaka's model is limited to the range of low steam pressure where the saturated steam can be treated as an ideal gas so that the ambient fluid surrounding the spray droplets is considered as an ideal–gas mixture composed of saturated steam and air. In this study, the transient temperatures of spray droplets when they impinge on the inner surface of pressurizer vessel wall are determined by using the computer code DROPHMT developed by the present authors. The code was designed to calculate the heat and mass transfer rates to a spray droplet moving in a space of real–gas mixture composed of saturated steam and noncondensable hydrogen gas at very high pressure. And the thermal boundary conditions at the inner surface of vessel wall which are governed by the behaviours of the saturation temperature of steam and the spray droplet temperature and velocity at the vessel wall

are mathematically described using the theoretical and empirical correlations for the heat transfer process during the Inadvertent Auxiliary Spray transient. Finally, the transient temperature distributions in the vessel wall are determined by using the general engineering analysis computer code ANSYS [3] and the typical calculated results are presented.

2. Analysis

2.1 Analysis Model

For the simplification of thermal analysis, neither the manway and any of the nozzles welded to the upper head of vessel is included in the analysis model, since they are located far from the region of upper shell exposed to spray flow in which the most severe temperature gradients are experienced, and the presence of instrument nozzles welded to the upper shell is ignored because they are too small in size compared to the upper head and shell. Also, the presence of any cladding on the vessel wall is not included in the thermal analysis since the cladding is 10% or less of total thickness of the wall. The material of vessel wall (Carbon steel, SA-533 Grade A-C12) is assumed to be isotropic and homogeneous. The space above the water surface in the pressurizer is filled with a real-gas mixture composed of the high pressure saturated steam and the noncondensable hydrogen gas. The entire wall of the pressurizer is assumed to be maintained initially at the same uniform and constant temperature as that of the real-gas mixture occuping the pressurizer interior space. The geometrical and thermal axisymmetry of the pressurizer vessel wall resulted in the consequence of above simplifications and assumptions indicates that it will suffice to examine the two-dimensional temperature distributions, in both axial and radial directions, within the region ABCDD′C′B′A′(Fig. 1).

2.2 Thermal Boundary Conditions

When the spray is activated, the temperature and mass of the droplets increase due to both convection from the ambient gas mixture and steam condensation as the droplets travel from the spray nozzle to the inner surface of vessel wall, and the total pressure and temperature of real-gas mixture decrease. The inner surface of vessel wall for the spray duration is divided into the natural convective boundary region exposed to the saturated steam-hydrogen gas mixture and the forced convective boundary region exposed to the spray droplets. The thermal boundary conditions subjected to the analysis model for the Inadvertent Auxiliary Spray transient, which greatly affect the type and amount of heat transfer to portions of the model are considered as follows;

(1) Natural convective boundary condition at hot wall surface exposed to cool gas mixture:

A state of natural convective heat transfer is considered to exist between the ambient real-gas mixture and the inner surface of entire upper head and the portion of upper shell, which are in contact with the real-gas mixture during the spray transient. For this kind of boundary condition, because the thermally induced fluid motion is found to be turbulent, the convective heat transfer coefficient is given by the following correlation [4,5] expressed in terms of fluid properties.

$$\frac{h_1 L}{k_f} = 0.13 \left[\frac{L^3 \rho^2 g \beta (T_w - T_v)}{\mu^2} \frac{C_p \mu}{k} \right]_f^{1/3} \quad (1)$$

Throughout this paper the subscript f will be used to indicate quantities which are evaluated at the average of the wall temperature and the temperature of surrounding fluid outside of the thermal boundary layer.

(2) Forced convective boundary condition at hot

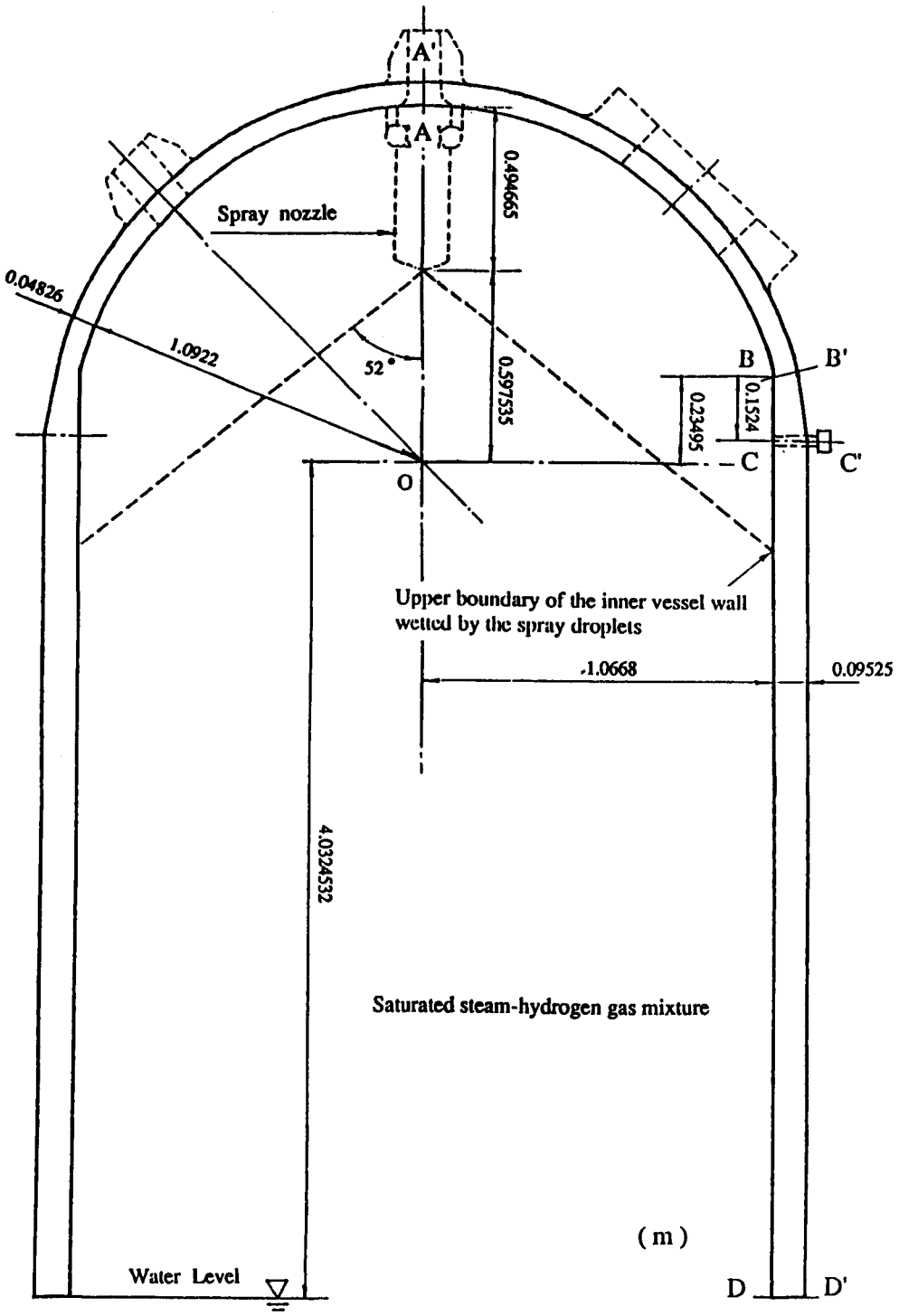

Fig. 1 Configuration of the Pressurizer Vessel.

wall surface exposed to cool spray:

The forced flow of water droplets through the spray nozzle indicates that forced convective heat transfer exists in region of vessel interior wall where the spray impinges on and flows down. If the droplet velocity and at the vessel wall and the velocity of the fluid flowing down the vessel wall are known, the forced convective heat transfer coefficient at the boundary surface can be determined by an available correlation. Because of the difficulties in describing a realistic analysis model and analyzing the thermal-hydraulic phenomena, a simplified model of an inclined plane where the fluid flows down is selected to determine the velocity of the sprayed water flowing down the vessel wall. From the solution of simultaneous equations for the asymptote film thickness and average velocity of the film, the following expression for the average velocity of the fluid flowing down a vertical wall can be derived[6,7].

$$V_{avg} = \left\{ \left[\frac{gQ}{0.0284p} \right] \left[\frac{\rho Q}{\mu p} \right]_l^{1/4} \right\}^{1/3} \quad (2)$$

where

p=width of the plate or perimeter of the vessel interior wall wetted by the spray flow.

Q=flow rate of the fluid.

and the subscript 1 denotes quantities evaluated at the temperature of free stream outside the fluid boundary layer. The free stream velocity of fluid flowing down the vessel interior wall may then be given by

$$V_l = \frac{8}{7} V_{avg} \quad (3)$$

Having the computer code for calculating the heat and mass transfer rates to droplets in the pressurizer and the derived expression for the velocity of fluid flowing down the vessel wall, sufficient data are available for modeling the process of heat transfer by forced convection in the region of the vessel interior wall exposed to spray flow. An appropriate correlation for the forced convective heat transfer due to turbulent flow parallel to a vertical wall is found in reference[8] as

$$\frac{h_2 L}{k_l} = 0.036 \left(\frac{C_p \mu}{k} \right)_l^{0.43} \left(\frac{\rho V_l L}{\mu} \right)_l^{0.8} \left(\frac{\mu_l}{\mu_w} \right)^{0.25} \quad (4)$$

where V_1 is the droplet velocity at the time ot impingement or the velocity of fluid flowing down the vessel wall whichever is greater, because the higher V_1 is, the more conservative the result solutions for the transient responses of the temperature gradients and thermal stresses in the vessel wall are.

(3) Filmwise condensation boundary condition at cool wall surface exposed to hot gas mixture:

After the end of spray period, the saturated steam at a higher temperature than the vessel wall temperature is in contact with the entire surface of model. Condensation of the saturated steam on the vessel wall can be mathematically described by an appropriate model for film condensation of a single vapor on vertical flat plates. Since dropwise condensation can be expected only under carefully controlled conditions, only a filmwise condensation model is employed. The Reynolds number of condensate film can be expressed as

$$\mathrm{Re} = \frac{4}{3} \left[\frac{4kL(T_v - T_w)\, \rho^{5/3} g^{1/3}}{\mu^{5/3} (\rho_f - \rho_v) H_{fg}} \right]_f^{3/4} \quad (5)$$

Motion of the condensate film becomes turbulent when its Reynolds number exceeds a critical value of about 2000. The recommended correlations for filmwise condensation[9] are as follows:

for laminar flow;

$$h_3 = 1.13\left[\frac{k^3\rho(\rho_f-\rho_v)gH_{fg}}{\mu L(T_v-T_w)}\right]_f^{1/4} \quad (6)$$

for turbulent flow;

$$h_3 = 0.0077\,\mathrm{Re}^{0.4}\left[\frac{k^3\rho^3 g}{\mu^2}\right]_f^{1/3} \quad (7)$$

(4) Insulated boundary condition:

It is assumed that the boundaries of model other than the inner surface of vessel wall, that is, the outer surface and both of the end boundaries, are perfectly insulated. Thus no heat is transferred across the boundaries.

2.3 Heat and Mass Transfer to a Spray Droplet

Consider the introduction of a cold water droplet of radius R_o and initial bulk temperature T_{lmo} into the saturated steam–hydrogen gas mixture space in a PWR pressurizer. The droplet is projected with an initial velocity W_o and at an angle θ_o with respect to the vertical direction, as depicted schematically in Fig. 2. The ambient pressure P_∞, the corresponding saturation temperature T_∞, and the mass fraction of noncondensable $W_{g\infty}$ are taken to be prescribed. The spray droplet is colder than the mixture. Thus steam condensation occurs on the droplet surface and the spray droplet grows as it travels in the mixture space. The condensation heat and mass transfer caused by the steam concentration difference between the ambient mixture and the gas–liquid interface. Hence the concentration of noncondensable hydrogen gas in the mixture may affect the heat and mass transfer rates to the spray droplet during the time of flight even when the concentration of noncondensable is very small. In this study, the heat transfer and motion of the spray droplets are theorectically formulated assuming that the moving spray droplets maintain the spherical shape, the drag phenomena are those for rigid spheres, and the radiation heat transfer to the droplet from the mixture is ignored. The total heat transfer from the mixture to the droplet surface is made up of the condensation heat transfer component and the convective heat transfer component caused by the temperature difference between the ambient mix-

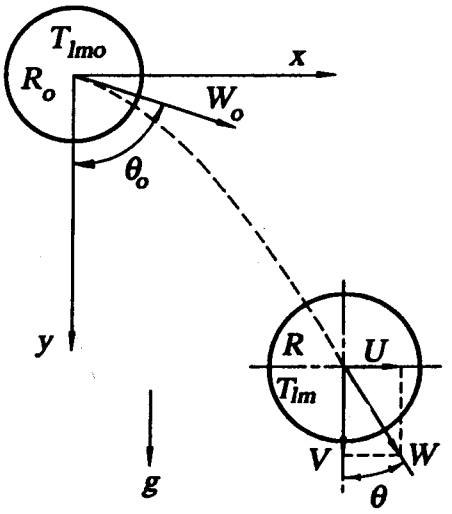

Fig. 2a Schematic of a Spray Droplet Model.

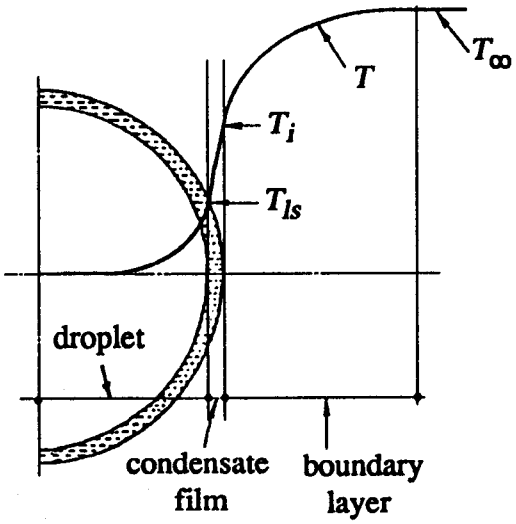

Fig. 2b Calculation Model of Film Condensation of a Droplt [2].

ture and the condensate liquid at the gas–liquid interface. Since the ambient fluid surrounding the droplets is a real–gas mixture composed of saturated steam and hydrogen gas at high pressure, the thermophysical properties of the environmental fluid is estimated by applying the concept of the compressibility factor and using appropriate correlations and experimental results. The mathematical basis of the DROPHMT code can be described in detail as follows;

The equations of motion for a spray droplet can be written as

$$\frac{dU}{dt} = -C_D A\rho_g \frac{WU}{2m} - \frac{U}{m}\frac{dm}{dt} \tag{8}$$

and

$$\frac{dV}{dt} = g\frac{(\rho_l - \rho_g)}{\rho_l} - C_D A\rho_g \frac{WV}{2m} - \frac{V}{m}\frac{dm}{dt}$$

The mass balance equation is given by

$$\frac{d}{dt}\left(\frac{4}{3}\pi\rho_l R^3\right) = 4\pi R^2 m_f \tag{10}$$

where m_f denotes the mass flux expressed by

$$m_f = \rho_v \beta (W_{gi} - W_{g\infty}) \tag{11}$$

and the mass transfer coefficient β [2] estimated from

$$\mathrm{Sh} = (2 + 0.60\,\mathrm{Re}_d^{1/2}\,\mathrm{Sc}^{1/3}) \times \left[1.39\left(1 + \frac{W_{g\infty}}{W_{gi}}\right)^{-0.48}\left(\frac{W_{gi}}{W_{g\infty}}\right)^{0.52} W_{gi}^{-1}\right] \tag{12}$$

The total heat flux q should be equal to film condensation heat flux expressed by the product of film condensation heat transfer coefficient h_f and temperature differnce between the gas–liquid interface and the droplet surface, $(T_i - T_{ls})$. Hence, the heat balance equation at the gas–liquid interface is given by

$$\begin{aligned} q &= m_f H_{fg} + h_{cv}(T_\infty - T_i) \\ &= h_f (T_i - T_{ls}) \end{aligned} \tag{13}$$

where the convection heat transfer coefficient h_{cv} [10] is obtained from

$$\mathrm{Nu} = 2 + 0.60\,\mathrm{Re}_d^{1/2}\,\mathrm{Pr}_g^{1/3} \tag{14}$$

and the heat transfer coefficient of condensate film h_f [2] is obtained from

$$\mathrm{Nu} = 0.986\left(1 + \frac{\mathrm{Pr}_l}{R_h H}\right)^{1/3}\mathrm{Re}_d^{1/2} \tag{15}$$

The vapor pressure at the gas–liquid interface can be expressed by

$$\frac{P_{vi}}{P_t} = \frac{(1 - W_{gi})}{1 - W_{gi}\left(1 - \frac{Z_g M_v}{Z_v M_g}\right)} \tag{16}$$

where the interface temperature is the saturation temperature of steam corresponding to P_{vi}. The thermal and physical properties of the condensate liquid and the environment fluid are calculated from the following reference temperatures [11].

$$T_{ref} = T_{ls} + 0.31(T_i - T_{ls}) \tag{17}$$

$$T_{oref} = T_i + 0.31(T_\infty - T_i) \tag{18}$$

The heat balance equation of complete mixing droplet model is

$$\frac{\rho_l C_{pl}}{3}\frac{d}{dt}(R^3 T_{lm}) = R^2 q \tag{19}$$

with initial condition $T_{lm} = T_{lmo}$, and T_{lm} is identified with the droplet surface temperature T_{ls}.

The governing equation of non–mixing droplet model is given by

$$\rho_l C_{pl}\frac{\partial T_l}{\partial t} = \frac{1}{r^2}\frac{\partial}{\partial r}\left(k_l r^2 \frac{\partial T_l}{\partial r}\right) \tag{20}$$

with the initial condition $T_1=T_{lmo}$, and the related boundary conditions are expressed by

$$\left.\frac{\partial T_l}{\partial r}\right|_{r=0}=0 \tag{21}$$

$$k_l\left.\frac{\partial T_l}{\partial r}\right|_{r=R}=q \tag{22}$$

where the interface temperature T_i becomes the droplet surface temperature T_{ls} in the calculation for next subsequent time step.

2.4. Thermal and Physical Properies of Mixture

The behavior of a real gas is expressed using the compressibility factor Z as

$$Z=\frac{P\bar{V}}{\bar{R}T} \tag{23}$$

or using the acentric factor ω, then

$$Z=Z^{(0)}(T_r,P_r)+\omega Z^{(1)}(T_r,P_r) \tag{24}$$

where $T_r=T/T_c$ and $P_r=P/P_c$, the functions $Z^{(0)}$ and $Z^{(1)}$ are obtained from Lee and Kesler's results [12]. As stated above, the compressibility factor is governed by the reduced temperature, reduced pressure and acentric factor. The physical properties for the mixture of saturated steam and hydrogen gas at high pressure are calculated by the use of pseudocritical values. The pseudocritical values of mixture are then obained from the following equations.

$$T_{cm}=\sum_i y_i T_{ci} \tag{25}$$

$$\bar{V}_{cm}=\sum_i y_i \bar{V}_{ci} \tag{26}$$

$$Z_{cm}=\sum_i y_i Z_{ci} \tag{27}$$

$$P_{cm}=\frac{Z_{cm}\bar{R}T_{cm}}{\bar{V}_{cm}} \tag{28}$$

where y_i is mole fraction of each component, and the molecular weight and acentric factor of mixture are given by

$$M_m=\sum_i y_i M_i \tag{29}$$

$$\omega_m=\sum_i y_i \omega_i \tag{30}$$

Density

The density ρ_m and reduced density ρ_{rm} of the gas mixture expressed by the followings may be determined by the equation of state and the expression for Z_m.

$$\rho_m=\frac{1}{v_m}=\frac{M_m}{\bar{V}_m} \tag{31}$$

$$\rho_{rm}=\frac{\rho_m}{\rho_{cm}}=\frac{\bar{V}_{cm}}{\bar{V}_m} \tag{32}$$

Thermal conductivity

The thermal conductivities of all gases increase with pressure, and most of all the correlations describing the effect of pressure on the thermal conductivity are based on the following correlating technique suggested by Vargaftik[13].

$$k_m-k_m^{\circ}=f(\rho_{rm}) \tag{33}$$

In this equation, the difference between thermal conductivity at high pressure and that at low pressure is a function of reduced density. Stiel and Thodos [14] suggest correlations for the function $f(\rho_{rm})$ as

$$f(\rho_{rm})=14.0\times10^{-8}\{\exp(0.535\rho_{rm}-1)/\Gamma_m Z_{cm}^5\} \quad \cdots\cdots (\rho_{rm}<0.5) \tag{34}$$

$$f(\rho_{rm})=13.1\times10^{-8}\{\exp(0.67\rho_{rm}-1.069)/\Gamma_m Z_{cm}^5\} \quad \cdots (0.5<\rho_{rm}<2.0) \tag{35}$$

$$f(\rho_m) = 2.976 \times 10^{-8}\{\exp(1.155\rho_{sm} + 2.016)/\Gamma_m Z_{cm}^5\} \cdots (2.0 < \rho_{rm} < 2.8) \quad (36)$$

where Γ_m is given by

$$\Gamma_m = \frac{T_{cm}^{1/6} M_m^{1/2}}{P_{cm}^{2/3}} \quad (37)$$

The thermal conductivity of mixture at low pressure is obtained by Brokaw's correlantation [15],

$$k_m = S k_{mL}^{\circ} + (1-S) k_{mR}^{\circ} \quad (38)$$

where

$$k_{mL}^{\circ} = \sum_i y_i k_i^{\circ} \quad (39)$$

$$\frac{1}{k_{mR}^{\circ}} = \sum_i \frac{y_i}{k_i^{\circ}} \quad (40)$$

and Brokaw factor S is given in Table 1.

Table 1. Variation of the Brokaw Factor S with Composition of Light Component

Mole fraction light component	Factor S for eq.(38)	Mole fraction light component	Factor S for eq.(38)
0.	0.32	0.6	0.50
0.1	0.34	0.7	0.55
0.2	0.37	0.8	0.61
0.3	0.39	0.9	0.69
0.4	0.42	0.95	0.74
0.5	0.46	1.0	0.84

Specific heat at constant pressure

In order to determine the specific heat at constant pressure of a gas mixture, the molar specific heat at constant pressure must be first evaluated by

$$C_{pm}^{\circ} = \sum_i y_i C_{pi}^{\circ} \quad (41)$$

Eq.(41) applies to an ideal gas, and the specific heat at constant pressure of real gas is related to the value in the ideal gas state, at the same temperature and composition,

$$C_{pm} = C_{pm}^{\circ} + \Delta C_{pm} \quad (42)$$

where ΔC_{pm} is a residual specific heat at constant pressure ; it can be determined by taking the partial derivative of enthalpy departure at constant pressure and composition.

$$\Delta C_{pm} = \frac{\partial}{\partial T}(H - H^{\circ})_{T,\,comp} \quad (43)$$

By the use of reduced temperature and pressure, ΔC_{pm} can be calculated from the Lee–Kesler method[12].

$$\Delta C_{pm} = (\Delta C_{pm})^{(0)} + \omega(\Delta C_{pm})^{(1)} \quad (44)$$

Viscosity

The viscosity of a mixture at high pressure is calculated from the following correlation suggested by Dean and Stiel[16],

$$(\mu_m - \mu_m^{\circ})\xi_m = 1.08\{\exp(1.439\rho_{rm}) - \exp(-1.111\rho_{rm}^{1.858})\} \quad (45)$$

where ρ_{rm} is reduced density, and ξ_m is given by

$$\xi_m = \frac{T_{cm}^{1/6}}{M_m^{1/2} P_{cm}^{2/3}} \quad (46)$$

The viscosity of a mixture at low pressure is calculated by Wilke's method[17],

$$\mu_m^{\circ} = \sum_i \frac{y_i \mu_i^{\circ}}{\sum_j y_j \phi_{ij}} \quad (47)$$

where

$$\phi_{ij} = \frac{\{1 + (\mu_i^{\circ}/\mu_j^{\circ})^{1/2}(M_j/M_i)^{1/4}\}^2}{\{8\ (1 + M_i/M_j)\}^{1/2}} \quad (48)$$

$$\phi_{ij} = \frac{\mu_i^\circ M_i}{\mu_j^\circ M_j}\phi_{ji}$$

Mass diffusivity

The mass diffusivity of a mixture is calculated from the correlation including the terms of the atomic diffusion volumes that is proposed by Fuller et al.[18].

$$D^\circ = \frac{1.013 \times 10^{-7} T^{1.75}\{(M_i + M_j)/M_i M_j\}^{1/2}}{P\{(\Sigma V)_i^{1/3} + (\Sigma V)_j^{1/3}\}^2} \quad (50)$$

By introducing the values of the atomic diffusion volumes, $(\Sigma V)_v = 12.7$ and $(\Sigma V)_g = 7.07$, and those of the molecular weight, $M_v = 18.015$ and $M_g = 2.016$, into the above equation, there follows

$$D^\circ = 4.16037 \times 10^{-9} T^{1.75}/P \quad (51)$$

Since this equation is valid at low pressure, the mass diffusivity at high pressure is calculated from the following correlation suggested by Dawson et al.[19].

$$\frac{D\rho}{(D\rho)^\circ} = 1 + 0.053423\rho_r - 0.030182\rho_r^2 - 0.029725\rho_r^3 \quad (52)$$

2.5 Calculation Procedure

The clculation procedure of the computer program DROPHMT is summarized as follows;

(1) The calculations are started by specifing the time step size. The specified time step must be sufficiently small in order that all the physical properties can be considered to be constants over each time interval. The time step size used in this study is 10^{-5} s which was shown to be optimum value through preliminary study.

(2) Guess an arbitrary value of mass fraction of noncondensable hydrogen gas at the gas–liquid interface W_{gi}.

(3) Determine the partial pressure of saturated steam at the interface P_{vi} corresponding saturation temperature of steam at the in terface T_i by using equation(16).

(4) Evaluate the physical properties of both condensate liquid and ambient fluid at the reference temperatures, T_{ref} and T_{oref}, determined from equation (17) and (18), respectively. The physical properties of saturated steam–hydrogen gas mixture are evaluated by using the correlations (23)~(52).

(5) Evaluate the condensation mass flux m_f, convective heat transfer coefficient h_{cv}, and condensation heat transfer coefficient h_f from equations (11), (12), (14) and (15).

(6) Check whether the calculated values of T_i, m_f, h_{cv} and h_f satisfy the following convergence criteria which is based on the heat balance equation (13).

$$\left| \frac{m_f H_{fg} + h_{cv}(T_\infty - T_i) - h_f(T_i - T_{ls})}{\mathrm{MIN}[m_f H_{fg} + h_{cv}(T_\infty - T_i),\ h_f(T_i - T_{ls})]} \right|$$

where MIN [A, B] denotes the smaller of A and B. The value of relative error ϵ specified in this study is 10^{-4} If the convergence criteria is not satisfied, return to step (2) with new guessed value of W_{gi}, and repeat the same procedure by the secant method until a converged value of W_{gi} is obtained.

(7) With the converged values of T_i, m_f, h_{cv} and h_f, corresponding to the converged value of W_{gi}, the total heat flux q is determined from equation (13).

(8) For the time interval with specified one time step size, the initial and/or boundary conditions necessary for solving the equations (8), (9), (10), (19) and (20) are available from the results of previous calculations. The velocities

U and V of droplet and its related trajectory are obtained from equation (8) and (9) by using the Runge–Kutta method. The solutions R and T_{lm} are straightforward since the equations (10) and (9) are ordinary differential equations. The solution of temperature distribution in the non–mixing droplet model is obtained from equation (20) by using finite difference method. The partial differential equation (20) is integrated over control volumes to obtain the finite difference equations formulated in the DROPHMT code. For the integration of the equation (20) over a time interval, a fully implicit formulation is employed. The resulting finite difference equations are solved by using the Tri–Diagonal Matrix Algorithm. The number of grids for non-mixing droplet model in radial direction used in this study is 101 which was shown to be optimum through preliminary study. All the calculation results obtained in the present calculation step are to be specified as the initial conditions of the differntial equations to be solved over next subsequent time interval.

(9) Return to the calculation step (2), and repeat the whole procedure for next time interval until the droplet reaches thermal equilibrium with the ambient fluid.

3. Calculated Results and Discussion

3.1 Transient Temperature of Spray Droplet

Considering the most conservative case of the Inadvertent Auxiliary Spray transient, the basic data for calculating the transient temperature and size of a spray droplet using the computer program DROPHMT are as follows;

Initial pressure and temperature in the pressurizer=155.13 bar, 345℃

Temperature of the spray water at nozzle outlet =0℃

Flow rate of the spray water at nozzle outlet $=12.618\times10^{-3}$ m^3/s

Average initial diameter of spray droplet =5.5 mm

Spray transient time =300 s

Spray cone angle =104 deg.

Droplet elapsed time of flight $=1.703\times10^{-4}$ hr

Orifice diameter =82.6 mm

Hydrogen to saturated steam mass fraction $=2.405\times10^{-3}$

The above information has been provided by a manufacturer of pressurizer spray nozzles employed in some domestic nuclear power plants in operation. All other physical properties of saturated steam, hydrogen gas, water and the material of vessel wall are obtained from the references [20–23]. The DROPHMT program can calculated for both the complete mixing droplet model and the non–mixing droplet model. The complete mixing model and non–mixing model respectively provide the upper and lower bounds on droplet temperature at the time when the droplet impacts the vessel inner surface. The upper bound value is nonconservatively high and the lower bound value conservatively low.

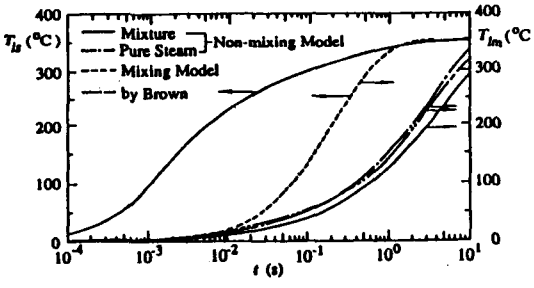

Fig. 3 The Variation of T_{lm} and T_{ls} with t.

Fig. 3 shows the transient responses of the volumetric mean temperatures T_{lm} and the droplet surface temperature T_{ls} for both droplet models

considered in the DROPHMT program. The volumetric mean temperature is obtained by the relation $T_{lm}=(1/v)\int T_l\, dv$. For the non-mixing model, the transient characteristics of the volumetric mean temperature of a droplet moving in pure steam space are analyzed, and the calculated results are compared with the case of a droplet in the real-gas mixture space. As a result, it is shown that the effect of the noncondensable hydrogen gas in the ambient fluid surrounding the droplet on the heat and mass transfer rates could not be ignored, even when the concentration of noncondensable gas in the steam space of the pressurizer is small. Brown[24] has predicted transient characteristics of volumetric mean temperature of water droplets experiencing condensation in pure steam space using a droplet model with no internal mixing, on the assumption that the surface temperature of a droplet immediately takes up, and remains at the steam temperature. Brown's results for droplet diameter of 5.5 mm are also depicted in Fig. 3. It is seen that these results parallel the present results for the non-mixing model.

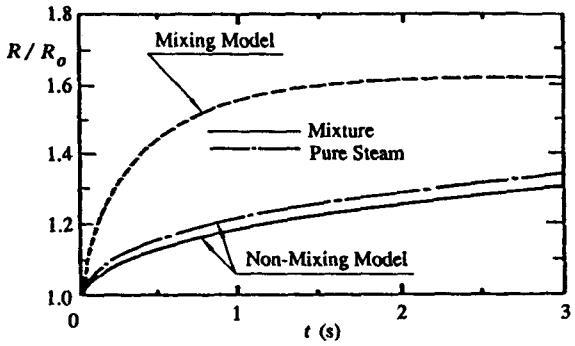

Fig. 4 Variation of R/R_0 with t.

In Fig. 4, the calculated results of growth rates of the mixing droplet model, non-mixing model in gas mixture space and non-mixing model in pure steam space are plotted. As expected from Fig. 3, the growth rate of a droplet due to steam condensation for the mixing model is larger than that for the non-mixing model. For the non-mixing model, the growth of a droplet in the real gas mixture of steam and the noncondensable hydrogen gas is smaller than that in pure steam because the external resistance on the heat and mass transfer to a droplet is increased by the presence of noncondensable gas.

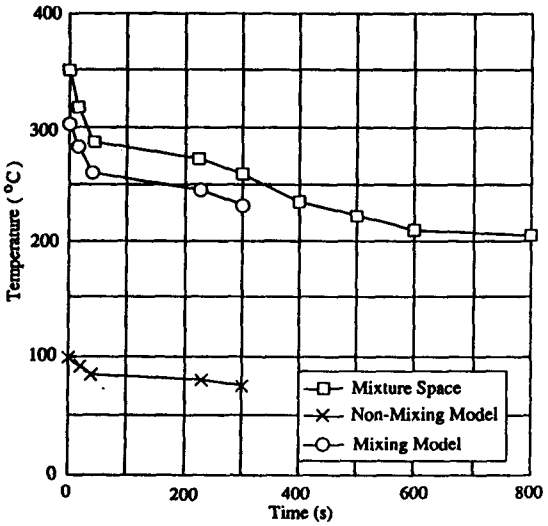

Fig. 5 Transient Volumetric Mean Temperature of a Spray Droplet at the Vessel Inner Surface and the Temperature History of the Mixture Space in the Pressurizer.

Fig. 5 shows the relations of the volumetric mean temperatures of both mixing and non-mixing droplet models when the droplet of which the trajectory line lies in the outer surface of spray cone impacts on the pressurizer vessel inner surface during the Inadvertent Auxiliary Spray transient. The curve of temperature history of the mixture space in the pressurizer for the Inadvertent Auxiliary Spray transient considered herein is plotted in Fig. 5. As shown in Fig. 5, the spray duration and the whole pressure transient period for the Inadvertent Auxiliary Spray transient are, respectively, 300 s and 800 s. This means that it takes 500 s from the end of spray period to the

beginning of pressure recovery in the pressurizer. In the thermal analysis for obtaining the transient temperature distributions in the pressurizer vessel wall during the Inadvertent Auxiliary Spray transient, the spray droplets are assumed to be rigid spheres with water properties in order to determine the droplet temperature conservatively. Thus, the droplet temperature at vessel wall used to determine the forced convective boundary condition at the region of the inner surface wetted by the spray droplets is calculated by the non–mixing droplet model.

3.2. Transient Temperature Distributions in the Pressurizer Vessel Wall

Necessary correlations and sufficient data for describing the thermal boundary conditions have been presented. It is assumed that the initial temperature of entire vessel wall is maintained uniformly at the same temperature of ambient mixture. Modification of the derived relations and application of the calculated results for use in the ANSYS computer code is straightforward. The transient responses of the temperature distribution in the pressurizer vessel wall during the spray transient are analyzed by solving the two–dimensional transient heat conduction equation with the related initial and boundary conditions.

The finite element thermal analysis is performed with the mesh shown in Fig. 6. The two –dimensional solution region to be considered herein are divided into a total of 960 axisymmetric 2–D isoparametric thermal solid elements with 1089 nodal points. The forced convective boundary surface wetted by spray flow is the portion FD. The remainder portion of wall inner surface ABF is natural convective boundary surface exposed to mixture. The mesh refinement near the inner surface of the shell as well as in the vicinity of the split thermal boundary FF′ separating the region FDD′F′F from the adjacent upper region is made in the nodalization as shown in Fig. 6 for the

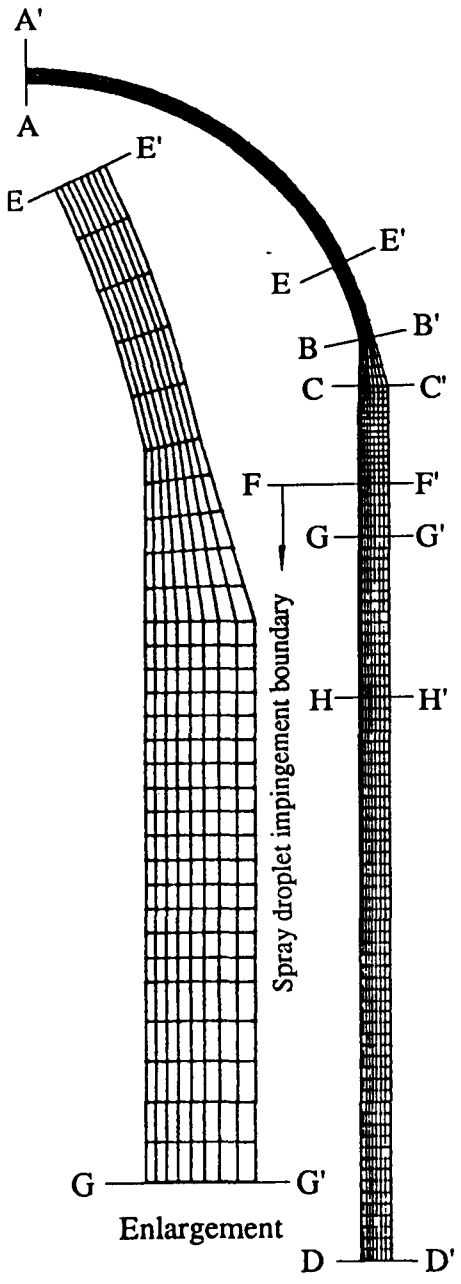

Fig. 6 Nodalization for Finite Element Analysis.

purpose of obtaining the temperature distribution as accurately as possible because the temperature gradients in those portions are expected to be significant. The material properties such as the thermal conductivity, density and heat capacity

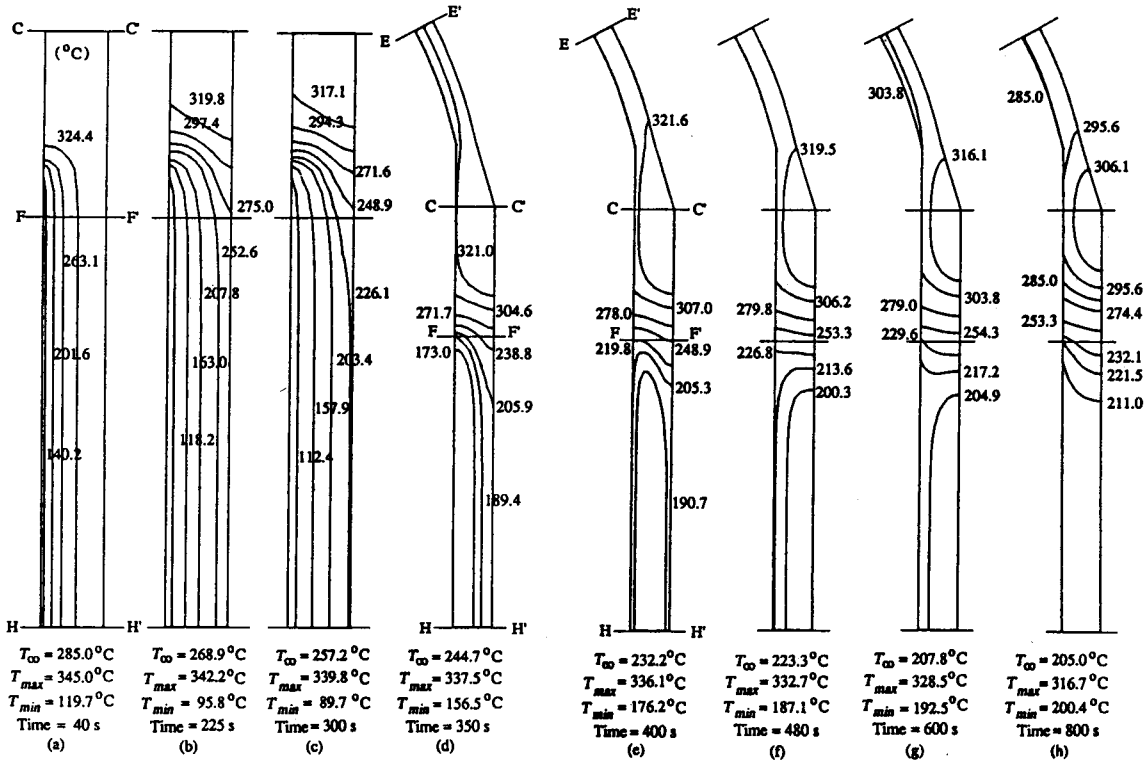

Fig. 7 Isotherms for the Transient Reponse of Vessel Wall.

used in the thermal analysis are considered as functions of temperature in the ANSYS program.

Isotherms in the pressurizer vessel wall, ploted from the transient temperature distributions calculated by the ANSYS code are presented in Fig. 7. The figure contains eight graphs corresponding, respectively, to the eight transient calculation results obtained at t=40 s, 225 s, 300 s, 350 s, 400 s, 480 s, 600 s and 800 s. The graphs show the isotherms in sectional wall regions where distinguishable temperature gradients are caused. Four graphs contained in Fig. 8 give the transient variations of transverse temperature distributions along the cross section EE′, CC′, FF′and HH′.

Figs. 7 and 8 show that for the whole transient period, the direction of heat flow in the entire wall, excepting the sectional region surrounding the position F which is the upper end of forced

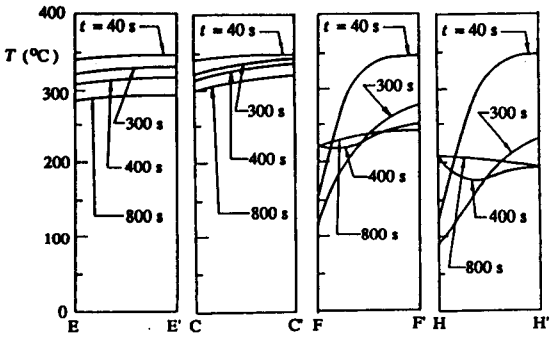

Fig. 8 The Transient Variations of Transverse Temperature Distributions Along the Cross Section EE′, CC′, FF′ and HH′.

convective boundary FD is nearly normal to the wall inner surface while in the sectional region surrounding the position F the heat flow in the axial direction is predominant, so that in the sectional region surrounding the split boundary FF′

the significant longitudinal temperature gradients are caused while in the region below the section FF′ the significant transverse temperature gradients are caused.

Further inspection of Figs. 7 and 8 indicates that the region affected directly by the spray flow is rapidly cooled during the spray period and is subjected to significant transient thermal loads over the whole period of the Inadvertent Auxiliary Spray transient. It is seen that the above results of the thermal analysis are consistent with representation of the input transient and have plausible physical meaning.

4. Conclusion

The methodology of determining the transient temperature distributions in the PWR pressurizer vessel wall for the Inadvertent Auxiliary Spray transient has been presented in this study. The transient temperatures of spray water droplets when they reach the inner surface of the vessel wall after travelling through the space of the saturated steam–hydrogen gas mixture from the spray nozzle have been predicted. The real–gas mixture is composed of saturated steam and hydrogen gas at high pressure. The analyses have been performed in a conservative manner using the computer program DROPHMT for calculating the heat and mass transfer rates to a spray droplet in a mixture composed of saturated steam and noncondensable hydrogen gas at high pressure. The calculated results of the droplet temperature at the wall inner surface and the velocity of the spray water flowing down the vessel wall which was estimated by a simplified analysis have been used to describe mathematically the forced convective heat transfer at the region of the wall inner surface region wetted by the spray. The transient temperature distributions in the pressurizer vessel wall have been obtained using the finite element program ANSYS, and the typical results obtained during the Inadvertent Auxiliary Spray transient have been provided. The results provided in this study may be employed as available input data for the analysis of transient thermal stress in the vessel wall.

Nomenclature

A = Cross–sectional area of droplet
C_D = Drag coefficient of sphere
C_P = Specific heat at constant pressure
d = Droplet diameter
g = Gravitational acceleration
H = Condensation parameter ($= C_{pl}(T_i - T_{ls})/H_{fg}$) or Enthalpy
H_{fg} = Latent heat of condensation
h = Heat transfer coefficient
k = Thermal conductivity
M = Molecular weight
m = Droplet mass
m_f = Mass flux per unit area
Nu = Average Nusselt number ($=hd/k$)
P = Pressure
Pr = Prandtl number ($=\nu/\alpha$)
q = Heat flux
R' = Drag force
$\bar{R}$ = Universal gas contant
Re_d = Reynolds number ($=\rho_g Wd/\mu_g$)
R_h = $\rho\mu$ ratio ($=[(\rho\mu)_l/(\rho\mu)_g]^{1/2}$)
r = Radial distance in spherical coordinate
S = Brokaw's factor
Sc = Schmidt number ($=\nu/D$)
Sh = Sherwood number ($=\beta d/D$)
T = Temperature
T_{max} = Maximum nodal point temperature
T_{min} = Minimum nodal point temperature
T_{oref} = Reference temperature of fluid within boundary layer
T_{ref} = Reference temperature of condensation film
t = Time
U = Horizontal velocity component

V =Vertical velocity component
$\bar{V}$ =Molar volume
v =Volume of droplet
W =Droplet velocity $(=(U^2+V^2)^{1/2})$
W_g =Mass fraction of gas
W_v =Mass fraction of vapour
x =Cartesian coordinate
y =Cartesian coordinate or Mole fraction
y_i =Mole fraction of each component
Z =Compressibility factor

Greek Symbols

β =Mass transfer coefficient or Thermal expansion coefficient
ϵ =Relative error
θ =Spray angle
μ =Dynamic viscosity
ρ =Density
ω =Acentric factor

Subscripts

c =Critical point
cv =Forced convection
f =Condensate film
g =Noncondensable gas or Gas phase
i =Interface
l =Liquid (Droplet)
m =Mean value or Mixture
o =Initial condition
r =Reduced value
s =Droplet surface
t =Total
v =Vapour
∞ =Ambient fluid
1 =Natural convection
2 =Forced convection
3 =Condensation

References

1. ASME Boiler and Pressure Vessel Code Section, "Rules for Construction of Nuclear Power Plant Components,"
2. Tanaka, M., "Heat Transfer of a Spray Droplet in a Nuclear Reactor Containment," Nucl. Tech., Vol.47, pp.268–281, (1980).
3. Peter C. Kohnke, ANSYS, Engineering Analysis System Rev. 4.3, Theoretical Manual, User's Manual, Swanson Analysis System Inc., Houston, (1987).
4. McAdams, W.H., Heat Transmission, 3rd ed., McGraw–Hill Book Company, New York, (1954).
5. Kreith, F., "Thermal Design of High Altitude Ballons and Instrument Packages," J. of Heat Transfer, 92C, pp.307–332, (1970).
6. Schlichting, H., Boundary Layer Theory, McGraw–Hill Book Company, New York, (1968).
7. Bird, R.B., et al., Transport Phenomena, Wiley & Sons Inc., (1966)
8. Whitaker, S., Elementary Heat Transfer Analysis, Pergamon, New York, (1976).
9. Özisik, M.N., Heat Transfer–A Basic Approach, 3rd ed., McGraw–Hill Book Company, New York, (1988).
10. Rantz, W.E., et al., "Evaporation from Drops," Chem. Eng. Prog., Vol.48, pp.141–173, (1952).
11. Sparrow, E.M., et al., "Forced Convection Condensation in the Presence of Noncondensables and Interfacial Resistance," Int. J.Heat Mass Transfer, Vol.10, pp.1829–1845, (1967).
12. Lee, B.I., and Kesler, M.G., "A Generalized Thermodynamic Correlation Based on Three–Parameter Corresponding States," AIChE J., Vol.21, No.3, pp.510–527, (1975).
13. Vargaftik, N.B., "Thermal Conductivities of Compressed Gases and Steam at High Pressure," Izv. Vses. Teplotekh. Inst., Moscow Enegetics Institute, (1951).
14. Stiel, L.I., and Thodos, G., "The Thermal Conductivity of Nonpolar Substances in the Dense Gaseous and Liquid Regions," AIChE

J., Vol.10, No.1, pp.26–30, (1964).
15. Brokaw, R.S., "Estimating Thermal Conductivities for Nonpolar Gas Mixtures," Ind. Eng. Chem., Vol.47, No.11, pp.2398–2400, (1955).
16. Dean, D.E., and Stiel, L.I., "The Viscosity of Nonpolar Gas Mixtures at Moderate and High Pressures," AIChE J., Vol. 11, No.3, pp.526–532, (1965).
17. Wilke, C.R., J.Chem. Phys., Vol.18, p.517, (1950).
18. Fuller, E.N., et al., Ind. Eng. Chem., Vol.58, No.5, P.18, (1966).
19. Dawson, R., Khoury, F., and Kobayashi, R., "Self–Diffusion Measurements in Methane by Pulsed Nuclear Magnetic Resonance," AIChE J., Vol.16, No.5, pp.725–729, (1970).
20. Meyer, C.A., et al., Thermodynamic and Transport Properties of Steam–ASME Steam Tables, ASME, New York, (1967).
21. Keenan, J.H., and Keyes, F.G., Thermodynamic Properties of Steam, John Wiley and Sons Inc., New York.
22. Reid, R.C., et al., The Properties of Gases and Liquids, 3rd ed., McGraw–Hill Book Company, New York, (1977).
23. Smithells, C.J., Metals Reference Book, 5ed., Butterworths, London & Boston, (1978).
24. Brown, G., "Heat Transmission by Condensation of Steam on a Spray of Water Drops," General Discussion on Heat Transfer, Institution of Mechanical Engineers, London, pp.49–52, (1951).